EMERGING HIGH-FREQUENCY (HF) AND **RELATED RADIO COMMUNICATIONS CONCEPTS** FOR ENDURING C³I ROLES IN A NUCLEAR

WAR ENVIRONMENT

Critical Issues in Nuclear Weapons Effects on

Propagation



C. B. Gabbard

R. E. LeLevier

R&D Associates

P.O. Box 9695

Marina del Rey, California 90291

1 June 1980

Topical Report for Period 5 January 1980-1 June 1980-

CONTRACT No. DNA 001-80-C-0069

THIS WORK SPONSORED BY THE DEFENSE NUCLEAR AGENCY UNDER RDT&E RMSS CODE B310080464 P990AXDB00157 H2590D.

DISTRIBUTION STATEMENT A

Approved for public releases

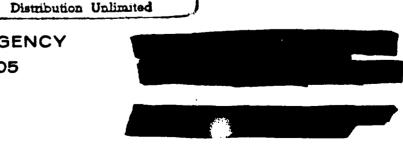
Prepared for

Director

DEFENSE NUCLEAR AGENCY

Washington, D. C. 20305

Rocament released mader the freedom et latermatine Act.



SECURITY CLASSIFICATION OF THIS PAGE (When Date Entered)

REPORT DOCUMENTATION	READ INSTRUCTIONS BEFORE COMPLETING FORM		
1. REPORT NUMBER	2. GOVT ACCESSION NO.	- RECIPIENT'S CATALOG NUMBER	
2 DNA 5551T ~ SAIV		,	
4 TITLE (and Subtitle) EMERGING HIGH-FREQU		5. TYPE OF REPORT & PERIOD COVERED	
RELATED RADIO COMMUNICATIONS CONCE		Dopical Report for Period	
C3I ROLES IN A NUCLEAR WAR ENVIRON	MENT,	5 Jan 80-1 Jun 80	
Critical Issues in Nuclear Weapons	Effects	PERFORMING ORG. REPORT NUMBER	
on Propagation		C RDA-TR-113212-001	
7 AuTHOR(x)		S CONTRACT OR GRANT NUMBER(s)	
C. B. Gabbard		}	
R. E. LeLevier		DNA 001-80-C-0069	
9 PERFORMING ORGANIZATION NAME AND ADDRESS		10 PROGRAM ELEMENT PROJECT, TASK AREA & WORK UNIT NUMBERS	
R & D Associates		THE TOTAL ONLY ADDRESS	
P. O. Box 9695		Subtask P990AXDB001-57	
Marina del Rey, California 90291			
11 CONTROLLING OFFICE NAME AND ADDRESS		12 REPORT DATE	
Director		1 June 1980 🔑	
Defense Nuclear Agency		13 NUMBER OF PAGES	
Washington, D. C. 20305		154	
14 MONITORING AGENCY NAME & ADDRESS(If differen	from Controlling Office)	15. SECURITY CLASS (of this report)	
		DOWNGRADING	
16 DISTRIBUTION STATEMENT (of this Report)			

17 DISTRIBUTION STATEMENT (of the abstract entered in Block 20, if different from Report)

18 SUPPLEMENTARY NOTES

This work sponsored by the Defense Nuclear Agency under RDT&E RMSS Code B310080464 P990AXDB00157 H2590D.

19 KEY WORDS (Continue on reverse side if necessary and identify by block number)

High frequency communications .
Radio communications ;
Groundwave communications ;
Command, control and communications (63)

1,20

ABSTRACT (Continue on reverse side if necessary and identify by block number)

This document summarizes the nuclear weapons effects on propagation issues that must be considered in judging the overall nuclear effects vulnerability of selected strategic C³ concepts envisioned to provide enduring C³I support in nuclear war. This document focuses on the propagation effects in bands ranging from MF to UHF, with emphasis on HF skywave propagation during and after periods of nuclear conflict. The report is composed of short contributions from selected experts in the field of nuclear propagation.

DD FORM 1473 EDITION OF 1 NOV 65 IS OBSOLETE

SECURITY CLASSIFICATION OF THIS PAGE (When Dare Entered)



SECURITY CLASSIFICATION OF THIS PAGE (When Dela Entered)

20. ABSTRACT (Continued)

effects (from RDA, SRI and Rand) and is intended to provide a guide for those asked to make system procurement decisions, in a complex and specialized but critical area.

O CONTRACTOR OF THE PARTY OF TH

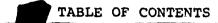
	
o del del Alconio di Località de	Ü
per eti	
Spinist of C	
5000	i
A-1	

SECURITY CLASSIFICATION OF THIS PAGE(When Date Entered)



This document presents a brief summary of the key points concerning the sensitivities of selected strategic C³ concepts to nuclear weapon effects on propagation. This document is intended to assist DoD decisionmakers in understanding and evaluating the potential endurance and performance of selected, emerging, ground and airborne strategic communication systems that would operate in the medium— to ultra-high-frequency radio bands in a general nuclear war.

This effort was sponsored by the Defense Nuclear Agency under Contract DNA001-80-C-0069 in response to numerous requests from DoD offices and the services on simple guidelines that (1) reflect the state-of-the-art understanding of nuclear weapon effects and (2) are useful in making system acquisition judgments.



Chapter		Page
	PREFACE	1
1	INTRODUCTION AND SUMMARY GUIDELINES	9
2	AN EMPIRICAL PERSPECTIVE ON HF SKYWAVE AND RELATED RADIO PROPAGATION DEGRADATION IN A NUCLEAR ENVIRONMENT	20
	Dr. R. E. LeLevier and Dr. C. B. Gabbard, R & D Associates	·
3	REVIEW OF PHENOMENOLOGY AND PREDICTIVE CAPABILITY IN HF SKYWAVE COMMUNICATIONS	55
	Dr. D. Neilson and Dr. E. Baumann, SRI International	
4	HF SKYWAVE COMMUNICATIONS ROLE AND THE NUCLEAR ENVIRONMENT	114
	Mr. W. Jaye, SRI International	
5	LOW DATA-RATE GROUND WAVE COMMUNICATIONS	132
	Dr. C. Crain, The Rand Componetion	

LIST OF ILLUSTRATIONS

rigure		Page
2-1	Riometer data following TEAK and ORANGE events	28
2-2	Riometer record for ALMA - 30 MHz	31
2-3	Riometer record for BIGHORN - 30MHz	31
2-4	Slant path attenuation versus time from daytime x-ray flash on the Soviet 22 and 28 October 1962 events	34
2-5	TEAK ionosonde data - Maui, H + 0 to H + 19 minutes	36
2-6	TEAK ionosonde data - Maui, H + 19 to H + 43 Minutes	37
2-7	TEAK ionosonde data - Midway Island, H + 0 to H + 19 minutes	38
2-8	TEAK ionosonde data - Midway Island, H + 19 to H + 43 minutes	39
2 -9	Map of vertical ionosonde stations	40
2-10	Critical frequency contours 0 minutes after KINGFISH	41
2-11	Critical frequency contours 3 minutes after KINGFISH	42
2-12	Critical frequency contours 10 minutes after KINGFISH	43
2-13	Critical frequency contours 32 minutes after KINGFISH	44
2-14	Critical frequency contours 60 minutes after KINGFISH	45
2-15	Critical frequency contours, 0 minutes after STARFISH	46
2-16	Critical frequency contours, 1 minute after STARFISH	47
2-17	Critical frequency contours, 10 minutes after STARFISH	48
2-18	Critical frequency contours, 32 minutes after STARFISH	49



LIST OF ILLUSTRATIONS (Continued)

Figure			Page
2-19	t.	Critical frequency contours, 60 minutes - after STARFISH	50
3-1		Oblique-incidence inograms showing (a) identification of raypaths and (b) oblique-vertical correspondence	63
3-2		Measured equinoctial propagation spectrum Ft. Monmouth to Palo Alto (1963-64)	65
3-3		Predicted and measured values of maximum observed frequency for Okinawa to Oahu path	66
3-4		Calculated and measured ionogram for Okinawa to Saigon path	67
3~5		Predicted and measured signal strength for 1300-km path	68
3~6		Geometry of raypath attenuation on a 1200-km path resulting from a near surface detonation	73
3~7		Ionospheric sounder paths for 1962 nuclear test series	77
3-8		Categories of bursts that cause HF absorption	79
3-9		Categories of bursts that may cause F-region changes	80
3-10		Distances at which prompt radiations cause blackout for various burst altitude/yield combinations	82
3-11		Prompt radiation effects—observed and computed—Canton to Hawaii path	83
3-12		Comparison of observed and predicted values of lowest observed frequency	86
3-13		Height/yield combinations required to maintain outage at distances within line-of-sight of the debris for the first 30 minutes	87



LIST OF ILLUSTRATIONS (Continued)

Figure			Page
3-14		Comparison of observed and computed gamma- ray induced absorption	88
3-15		One-way-vertical excess absorption at 15 MHz resulting from Beta, Gamma, and Prompt radiations—H + 15 min	89
3-16		fmin Behavior at Midway and Maui following TEAK	92
3-17		fmin Behavior at Midway and Maui following ORANGE	93
3-18		Riometer measurements at Midway and Maui following TEAK	94
3-19		Riometer measurements at Midway and Maui following ORANGE	95
3-20		fmin Behavior at Tomsk following October 1962 event	96
3-21		Virtual height and critical frequencies at Midway and Maui following TEAK	98
3-22		Transition from initial to acoustic-wave velocity	100
3-23		Geomagnetic field dependence of acoustic-gravity wave	101
3-24		Ionospheric wave position vs. time following check mate	102
3-25		Computed and-measured propagation spectrum— Canton to Rarotonga path	103
3-26		Equiangular scattering geometry	104
3-27		Paths and time durations of off-path modes resulting from high altitude ionization	105
3-28		Geomagnetic relationship on Canton to Hawaii and Midway paths and measured propagation spectrum	107
4-1		NMCS C ³ facilities—pre-hostilities	116
4-2	7	NMCS C ³ facilities—H + 33 min	117



LIST OF ILLUSTRATIONS (Continued)

Figure		Page
4-3	Geographical locations of low-altitude nudets over CONUS. Cumulative to H + 35 min	120
4-4	One-way-vertical absorption at 15 MHz—T = 10 min. 1 MT at 75 km	122
4-5	One-way-vertical absorption at 15 MHz— T = 1 hr. 1 MT at 75 km	123
4-6	One-way-vertical absorption at 15 MHz— T = 2 hr. 1 MT at 75 km	124
4-7	Potential region of communication from Omaha via field aligned ionization— single burst case	127
4-8	Potential region of communication from Omaha via field aligned ionization— all field lines	128
5-1	Comparative ground wave and ionospheric transmission	134
5-2	Ground wave basic transmission loss	136
5-3	CCIR quiet man-made noise levels (Ref. 2)	139
5-4	Signal to-noise ratio vs. frequency (ground wave tramission over land)	142
5 5	Signal-to-noise ratio vs. range—ground wave tramission over land	143

LIST OF TABLES

<u> Fable</u>		Page
2-1	Data Base	25
2-2	One-way vertical absorption, BIGHORN	32
2-3	One-way vertical absorption, ALMA	32
3-1	Perceptions of the survivability of HF communications systems	58
3-2	Major HF Nuclear effects codes	74
3-3	Predictability of the effects of various nuclear phenomena	81
4-1	Physical damage by blast summary	118
4-2	Duration of blackout—absorption only	126



For the purpose of providing initial insight into the nuclear weapon systems of interest, it is convenient to classify them according to the degree of dependence that radio propagation links have on the earth's ionosphere. This is quite simply because nuclear-weapon-induced disturbances in the earth's ionospheric medium are much more widespread, more persistent and less certain (in a prediction sense) than are nuclear-weapon-induced changes in the earth's atmosphere. For the system concepts mentioned earlier, the following categories will be used:

Concepts Dependent on Ionospheric Propagation

- Adaptive HF Communication Systems
- Meteor (Burst) Scatter Systems

Concepts Independent of Ionospheric Propagation

- Line-of-Sight Radio Networks (Airborne or Ground-Based Platform)
- Groundwave Communication Net orks

In the next two sections it will be seen that important points concerning the link vulnerabilities of concepts employing line-of-sight propagation and, to some extent, groundwave propagation are straightforward. Alternately, important conclusions concerning concepts employing ionospheric-dependent modes of propagation warrant supporting explanations. These explanations are then provided in subsequent chapters.

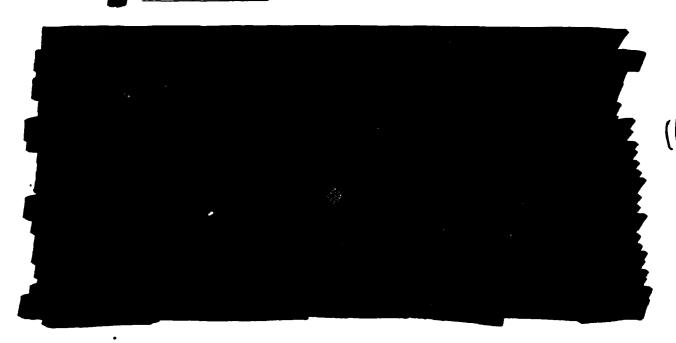
11



THE U.S. EXPERIENCE - A DATA BASE OVERVIEW 2.1

HF skywave propagation in a nuclear environment is by no means a clear-cut matter of poor performance. The viability of HF skywave in a nuclear environment has been and will continue to be a controversial issue in the C³ community. Although no compelling reason exists for providing herein an historical and detailed description of the many intercommunity quarrels and misconceptions that have emerged over the years, some perspective on the issue concerning the reliability of skywave communications is warranted. One of the more reasonable avenues toward understanding skywave problems in a nuclear environment is to examine the test data base itself. The following discussion [1] provides a succinct review of the U.S. experimental experience.

2.1.1 U.S. Data Base



22

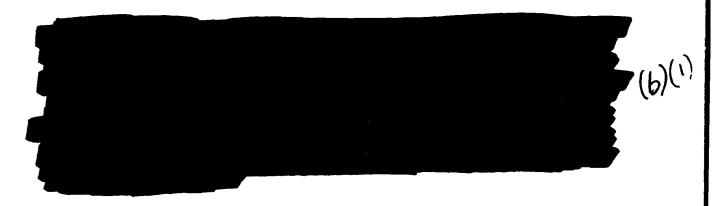
Pages 23 through 32 were deleted.

(b)(1) and (b)(3)

Prompt radiation from a high-altitude detonation (x-rays, neutrons and gamma-rays) can produce a level of ionization in the lower ionosphere that is sufficiently high that, after a certain amount of time, additional radiation will neither add appreciably to the ionization level nor lengthen its decay. The ionospheric electron density at a postburst time, t, is

$$N_e(t) \propto \frac{N_e(0)}{1 + \alpha N_e(0)t}$$

where N_e(o) is the initial electron density produced by the radiation pulse and α is the electron-ion recombination coefficient, which is of $O(10^{-7}~\text{cm}^3/\text{sec})$. If the condition $\alpha N_e(o)t >> 1$ is met, then N_e(t) becomes independent of N_e(o) after a time t (e.g., if N_e(o) $\sim 10^8~\text{e}^{-/\text{cm}^3}$, then N_e(t) is saturated after 1 sec).



2.2.2 F-Layer Depletion Effects





- 1. H. Foley et al., JASON Panel Report on the DNA Reaction
 Rate Program , Stanford Research Institute, Technical
 Report JSR-74-4, November 1975
- 2. R. Latter and R. E. LeLevier, <u>The Effects of Nuclear</u>
 Explosions on the Propagation of Electromagentic Waves
 The Rand Corporation, RM-2168, 1958
- 3. R. Latter and R. E. LeLevier, The PEAR Shot Corporation, RM-3081-PR, 1962a
- 4. R. Latter and R. E. LeLevier, Analysis of Two Explosions
 The Rand Corporation, RM-3082-PR, 1962B
- 5. R. E. LeLevier, The SWEG Report--Altitudes and Yields DASA-69-04291, 1968
- 6. W. S. Knapp, A Simplified D-Region Chemistry Model for Nuclear Environments DNA-2850T, General Electric Company-TEMPO, Center for Advanced Studies, April 1972
- 7. C. B. Gabbard, High Frequency (HF) Command and Control Communications (C³) in a Nuclear Environment R & D Associates, RDA-TR-221-NTA, October 1973
- 8. R. E. LeLevier, SWEG-1, A Report of the Special Weapons Effects Group, DASIAC SR-90, 6 March 1969,
- 9. R. J. Woodbury, Jr., Perturbation of HF Signals by Nuclear Detonations , Vol. 182, Sylvania Electronic System, EDL-M723, I September 1964
- 10. R. W. Hendrick, Jr., Nuclear Detonation Degradation of Over-the-Horizon Radars G. E. TEMPO, 67 TEMPO-88, August 1967
- 11. R. Latter and R. E. LeLevier, "Detection of Ionization Effects from Nuclear Explosions in Space," <u>Journal of</u> Geophysical Research, Vol. 68, No. 1643, March 1963.



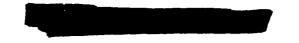


- 12. W. S. Knapp, private communication.
- 13. J. B. Lomax, D. L. Nielson and R. A. Nelson, <u>Contour</u>

 Maps of Critical Frequency Illustrating Effects on the

 Ionosphere of High-Altitude Nuclear Tests

 Report 1657, Stanford Research Institute, November 1965



CHAPTER 3. REVIEW OF PHENOMENOLOGY AND PREDICTIVE CAPABILITY IN HF SKYWAVE COMMUNICATIONS

Dr. D. Neilson and Dr. E. Baumann*, SRI International

I INTRODUCTION

This paper is a general synopsis of our HF prediction capability in a nuclear environment. We review our ability to understand, model, and ultimately predict HF performance under ambient conditions and for each significant atmospheric effect produced by a nuclear weapon. Wherever possible, examples of specific weapon-induced degradation effects on HF measurements are compared with predictions. The predictions are then evaluated in terms of our ability to model the significant factors in ambient and the specific nuclear situations; uncertainties associated with the specific models are also identified.

The major objective of this paper is to identify situations in which:

- The prediction codes provide reasonably good estimates of expected performance.
- Major uncertainties exist in the models, and when these uncertainties have a major effect on prediction and system performance estimates.
- Srandard nuclear effects analysis techniques may not be appropriate for new-generation HF systems.

The scope of the HF prediction problem is outlined in Section II; also included is a summarization of the changes in perception of the utility of HF systems as a part of a survivable network since the high-altitude nuclear detonations in 1958. In Section III, our ambient HF predictive capabilities are addressed, and uncertainties that may significantly affect our evaluations of the performance of new-generation systems are identified. The available HF nuclear effects prediction codes, along with their major features, are identified in Section IV. Finally, predictions are compared with measurements in Section V for the weapons' mechanical and radiative outputs that have a significant effect on HF predictions.



Evaluation of the ability to predict HF performance in a nuclear environment requires (1) assessment of the prediction capabilities in a natural environment and (2) review and assessment of our understanding of the interactions of a nuclear detonation with the propagation radium. Prediction of ambient propagation conditions is in itself a formidable task: at least eight basic factors must be accounted for to adequately represent electron density profiles along a path. The ambient electron density exists in a delicate balance of electron and ion production mechanisms that is susceptible to day-to-day changes and differs greatly as a function of: (1) time of day, (2) season, (3) latitude, and (4) solar activity. The HF system performance predictions must also account for other factors relating to the specific propagation path: (5) length, (6) orientation, (7) location, and finally (8) the system characteristics.

Adequate representation of propagation conditions in the natural environment is very important to nuclear predictions because:

- The nuclear effects are superimposed on the background electron density profile.
- The background electron density profile provides the baseline for computing the ionospheric recovery from the radiative and mechanical effects of a nuclear detonation.

System performance predictions in the nuclear environment must account for the eight factors that control the ambient conditions and six additional factors concerning the burst: (1) altitude, (2) yield, (3) location with respect to the propagation path, (4) single or multiple burst, (5) type of weapon, and (6) time after burst. Thus, accounting for and modeling these 14 factors makes predicting HF performance in a nuclear environment a truly multidimensional problem.

A STAIR BURGER

III PREDICTION OF THE AMBIENT IONOSPHERE AND OF THE PROPAGATION CONDITIONS

A. Ionospheric Predictions

The veracity of HF propagation and system performance predictions depends critically on the validity of the ionospheric model that depicts the ambient electron density profile along a path.

Available ionospheric models range in complexity from those depicting a single electron density profile to those using a multiple parameter representation that is variable in time and space. Here, we attempt to focus on our prediction capabilities—ionospheric and propagation—and our ability to relate them to emerging problems of evaluating the potential performance of new-generation HF systems. A significant number of these problems center on our ability to model and predict the often rapidly changing ionospheric conditions in the auroral and polar regions.

One of the more comprehensive available ionospheric models has been developed by the ITS. The ITS model contains worldwide maps of for, M(3000)F2, foE, and fEs, which are provided as functions of local time, month, latitude, and sunspot activity. Scaled vertical-incidence for the model, recorded at hourly intervals at many stations throughout the world over extended periods of time, constitute the data base for this model. The model provides a good statistical representation of the monthly median E- and F-layer parameters and the median and decile values of fEs. Factors are available for adjusting the median F-region parameters to those at the upper decile value. A model describing the ionospheric conditions in the auroral and polar regions has been developed recently. This model has a somewhat larger high-latitude data base and provides greater detail of the fine-scale structured ionosphere that exists in those regions. Again, however, it largely represents monthly median conditions. The auroral model has recently been integrated into

the ITS model by SRI, and the combination probably provides the most comprehensive worldwide ionospheric model now available.

Since the available ionospheric models represent median ionospheric conditions, predictions of the maximum propagating frequencies are lower than actual 50 percent of the time. Variations between the decile values and the monthly median values of ionospheric parameters are on the order of 20 to 30 percent, even for magnetically quiet midlatitude conditions; they are thought to be even greater in the auroral, polar, and equatorial regions.

A number of physical phenomena produce the ionospheric variations that are translated into comparable changes in the HF propagation spectrum. The physical phenomena that produce upper decile ionospheric values are the result of enhanced solar flux, movements of ionization-e.g., traveling disturbances, ionospheric storms, and magnetic disturbances—and sporadic E. Unfortunately, the various phenomena produce ionospheric changes with significantly different temporal behavior and spatial extents. Changes resulting from increased solar flux are wide-spread, persistent, and correlated in time and space, while changes resulting from traveling ionospheric disturbances or sporadic E are expected to be somewhat local and decorrelated in time and space.

Estimating the degree of spatial correlation of the F-region variations is extremely important in the evaluation of network connectivity for the new-generation HF systems, because the network encompasses a large geographic area and separated links are relied on for redundancy. For example, the usefulness of the abnormally high frequencies for the advanced system may depend on the degree of spatial correlation of the upper decile frequencies. Careful treatment of the occurrence of higher frequencies is important in a network analysis because, particularly in nuclear situations, the higher frequencies are expected to provide the best, and in many situations the only, available communication channels for network connectivity.

1"]

B. Propagation Predictions

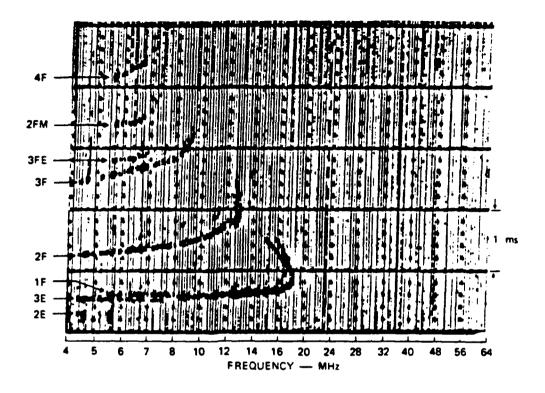
All general-purpose models for predicting nuclear effects on HF propagation and the resulting system performance represent a series of tradeoffs. One of the major tradeoffs in the propagation model is between computational costs and the need to preserve the detail provided by the ionospheric and nuclear effects models. Some propagation programs that match the detail of, say, the WEPH code require ray tracing to accurately portray the impact. If a large number of links and weapons are involved in the analysis, the computational costs become unaffordable. On the other hand, programs that can cope with the large number of links economically must simplify their approach to propagation and link analysis.

Historically, HF propagation predictions have centered on predicting the upper frequency of the propagation spectrum over a given path and, through estimating the signal-to-noise ratio at the receiver, the lowest frequency. Occasionally the predictions account grossly for the effects of multipath--a measure of the received signal's time dispersion-by predicting all successfully received rays and their corresponding signal strength.

Most HF propagation models associated with nuclear effects prediction use a parabolic representation of the electron density profile; this parabolic representation represents a compromise between computational speed, derived from ray equations having a closed form solution, and ray path accuracy. However, since the ionospheric models represent only median conditions anyway, results obtained with the parabolic representation appear adequate for most systems applications.

Much, if not most, of our present modeling of the ionosphere came from sweep-frequency pulse measurements, called ionograms, taken around the world. Usually taken at vertical incidence, these records have been translated into electron density profiles over time and space. Bistatic, or oblique, ionograms are similar and relatable, with some assumptions, to those taken at vertical incidence (Figure 1). Both vertical and oblique records were taken as diagnostic data during a number of nuclear tests. The oblique record principally shows the propagating





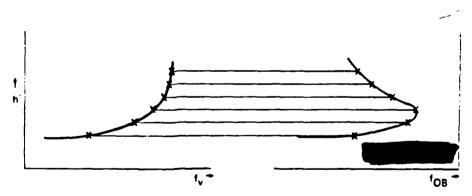


FIGURE 3-1 OBLIQUE-INCIDENCE IONOGRAMS SHOWING (a) IDENTIFICATION OF RAYPATHS AND (b) OBLIQUE-VERTICAL CORRESPONDENCE

spectrum between two points. Incidentally, it may indicate some aspects of the nuclear detonation itself. For example, absorption resulting from prompt or delayed radiation will affect the lower frequencies, while F-region waves or ionization will affect the higher frequencies. We will

refer to records of this type below. First, let us examine our ability to predict ionospheric behavior as it affects communication parameters.

C. Comparisons of Measurements with Predictions

The diurnal changes and the day-to-day variability in the measured propagation spectrum are illustrated in Figure 2 for a typical +000-km midlatitude path during an equinoctial month at the minimum of the solar cycle. Histograms show the percentage of time each frequency in the propagation spectrum was available for each two-hour time block. For example, in the 00 to 02 time block, frequencies between 8 and 15 MHz were available 100 percent of the time; the occurrence decreased to 80 percent at 18 MHz and to 5 percent at 24 MHz. The magnitude of the MUF variations from the median is indicated by the curve of predicted maximum frequency which is laid over the occurrence histograms. The measured frequencies exceed the predictions for all 12 time blocks, and frequencies as much as 10 MHz above the median would be available 10 percent of the time. Typical monthly variations of the observed maximum frequency about the median are shown in Figure 3 for the Okinawa to Oahu path. 13 The maximum variation occurred near 00 GMT, with a value of about = 9 MHz about the median frequency of 29 MHz. The predicted values of maximum observed frequency are also indicated on the figure; they are somewhat higher but generally consistent with the measured values.

A different and more detailed comparison between measurements and predictions is shown for the mid-latitude path from Okinawa to Saigon in Figure 4.14 There is excellent correlation between the predictions (indicated by an x) and the measurements (indicated by a box) for the propagating frequencies, raypaths, and the time-delay between the various rays. Although the good agreement between predictions and measurements cannot be considered typical, it presents strong evidence that limitations in the prediction accuracy are generally related to limitations in the ionospheric model rather than to those in the propagation model.

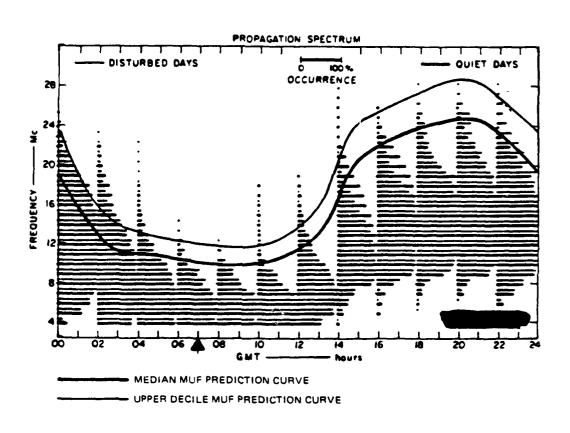


FIGURE 3-2 MEASURED EQUINOCTIAL PROPAGATION SPECTRUM FT. MONMOUTH TO PALO ALTO (1963-64)

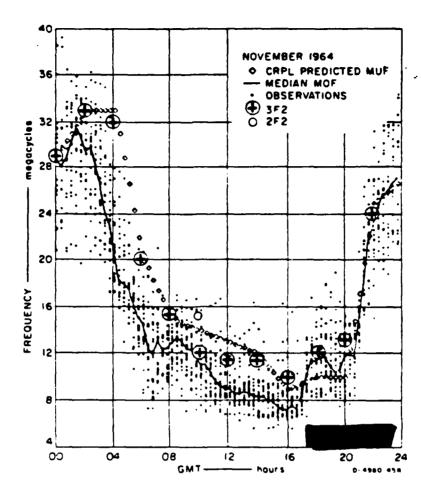


FIGURE 3-3 PREDICTED AND MEASURED VALUES OF MAXIMUM OBSERVED FREQUENCY FOR OKINAWA TO OAHU PATH

Another parameter important to communications is signal strength. Figure 5 shows an example of the predicted and average measured signal strength for a path from Illinois to Colorado. Because the measurements are CW signal strengths, the individual modes that contribute to the composite signal are unknown. A good comparison of calculated signal strength with measurements tends to validate the mode-of-propagation calculations as well as those of path losses.

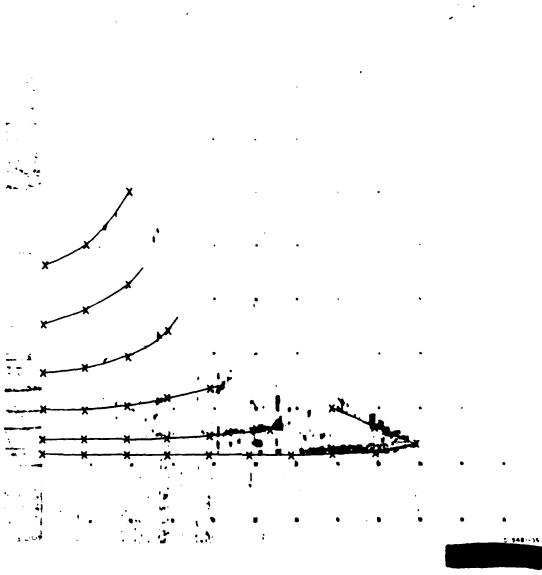


FIGURE 3-4 CALCULATED AND MEASURED IONOGRAM FOR OKINAWA TO SAIGON PATH

PREDICTED AND MEASURED SIGNAL STRENGTH FOR 1300-km PATH

IV NUCLEAR HF PREDICTION TECHNIQUES

A. General

Most of the energy (about 95 percent) of a nuclear explosion is released as prompt radiation at the instant of detonation. Prompt radiation consists of X-rays (about 70 percent), debris kinetic energy (about 25 percent), and neutrons (about 1 percent). The remaining 5 percent of the energy-called delayed radiation--is divided equally between gamma rays and beta particles and is released gradually as the decaying fission debris rises and expands.

Four major potential sources of degradation must be considered in analyzing HF performance in a nuclear environment:

- The early-time D-region signal absorption, resulting from prompt plus delayed radiation sources.
- The late-time D-region signal absorption, resulting from delayed garma ray and beta particle ionization.
- Changes in the propagating spectrum produced by traveling disturbances in the F-region.
- Increased scintillations and multipath from high-altitude ionization.

Although there is no clear-cut demarcation between "early times" and "late times," we loosely define the former as the time frame in which absorption owing to X-rays and gamma rays dominates.

Although the delayed radiation is only a small fraction of the total energy released by a nuclear detonation, it is the source of persistent HF signal absorption. Whereas the prompt radiations deposit their energy in a single impulse, the delayed radiation is emitted continuously as the fission debris undergoes radioactive decay. Its initial intensity depends on the fission yield, rather than the total yield, of the weapon, and it decreases as t^{-1.2}, or slightly faster tham inversely with time. As the debris rises and expands, the spatial extent of

ionization produced by delayed radiations increases. After the debris reaches its stabilization altitude, its distribution depends largely on atmospheric winds.



Nuclear Effects Prediction Codes

HF nuclear effects predictions generally entail the use of five complex physical models to account for the significant ionospheric, propagation and system parameters. There are a number of prediction programs available, and the five models have varying degrees of sophistication.

Some of the various models and their available options are:

- (1) Ionospheric models:
 - (a) Constant electron density profiles along a propagation path
 - (b) Varying profiles in time and space that represent monthly median profiles
 - (c) Specified (analytical) profiles

- (d) One or multiple parameters depicting major attributes of a profile
- (2) Propagation models
 - (a) Virtual geometry ray calculations for specified mode structures
 - (b) Raytracing techniques without limiting the mode structure
- (3) Noise model
 - (a) Worldwide noise maps
 - (b) Calculated noise values based on virtual noise sources
- (4) System model
 - (a) Path loss calculations
 - (b) Signal-to-noise ratios
 - (c) Signal characteristics, including estimates of signal distortions
- (5) Nuclear effects models
 - (a) Prompt radiation
 - (b) Delayed radiation
 - (c) Fireball/debris phenomenology
 - (d) Debris location
 - (i) Early times
 - (ii) Late times
 - (e) Ionospheric wave motions

It is useful at this point to discuss a few aspects of the development and evolution of the nuclear effects prediction models. The first comprehensive prediction model, termed WEPH, was developed in the early 1960s on the basis of empirical data collected during the 1958 and 1962 nuclear test series in the Pacific. As understanding of the interactions of a nuclear detonation with the surrounding medium has increased, WEPH has been routinely updated to reflect the current understanding. The updates reflect the work of many study groups that address specific phenomena relating to a nuclear detonation—i.e., fireball and debris phenomenology, atmospheric chemistry, heave, winds, striations, and clutter. The model's developed by the special studies generally entail the use of complex multispecies codes that model the physical processes

appropriate to a specific study. Such codes are extremely expensive to run and, accordingly, are not appropriate for typical systems analysis problems. To provide a useful systems analysis prediction code, the current version of WEPH uses analytic approximations with accuracies that are consistent with the current state of knowledge for each physical phenomenon.

Given that the nuclear effects model that one may use for a specific study represents the current state of knowledge, an HF prediction code must adequately represent the propagation conditions along a path to provide meaningful results. In contrast with predictions of systems that operate at frequencies that only propagate via line-of-sight, predictions of the HF raypath characteristics in a nuclear environment must consider the multiray property of HF propagation. This is particularly important when the burst-produced absorption region is small compared to the interray spacing, as illustrated in Figure 6. Three raypaths are shown connecting the transmitter to the receiver, but only two--the lF and 2F--intersect the nuclear-induced absorption region. Consequently, signals propagating via the 1E ray will be successfully received; no significant change in received signal strength is expected for the nuclear case, since under ambient conditions the signal strength is approximately comparable on the 1E and 1F raypath and only slightly lower on the 2F raypath.

The major HF nuclear effects prediction codes that are available through the DNA are listed in Table 2.15-19 Each code's design and complexity varies considerably and reflects the wide range of problems of HF predictions. Because of the wide range of HF problems, no attempts are made in this review to evaluate the merits of the various codes; instead, factors are identified that may affect the prediction results for certain classes of problems.

The primary purpose of the WEPH code is to model the interactions of single or multiple weapons with the surrounding medium. It is an integral part of the NUCOM, NUCOM-BREM and WRECS codes. WEPH provides one-way absorption estimates along a straight line. Thus, although-WEPH does not have an HF propagation model, the code can provide first-order

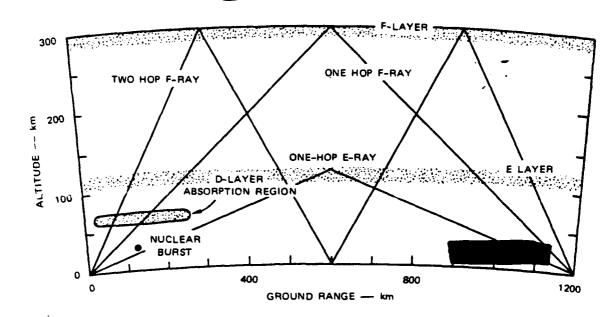


FIGURE 3-6 GEOMETRY OF RAYPATH ATTENUATION ON A 1200-km PATH RESULTING FROM A NEAR SURFACE DETONATION

system performance estimates for scenarios and situations in which absorption is the dominant nuclear-induced degradation--e.g., for massive laydowns, splead-debris situations, early-time X-ray situation.

The WRECS and HFNET codes were designed to compute the nuclear effects produced by many weapons on large networks. To accommodate the computational costs associated with large problems, each code implements different shortcuts in both the phenomenology and propagation models.

NUCOM, on the other hand, was designed to provide propagation and system performance estimates on single links at a level consistent with the results obtained from WEPH. Accordingly, the computational costs are somewhat greater.

Ambient ionospheric models are important to nuclear effects estimates for situations in which absorption does not dominate the results. HFNET and NUCOM both use versions of the ITS maps of coefficients of the E- and F-layer parameters mentioned in Section III-B. WRECS uses profiles that are functions of latitude and day/night conditions, and WEPH uses profiles that are a function of day/night conditions.

Table 3-2

MAJOR HE NUCLEAR EFFECTS CODES

ntion Noise System	Ambient (ITS) Limited	1 3-D Ambient (CCIR) Simple plus synchro-antenna tron plus cd receiver	Ambient (CCIR) Voice, FSK, antenna pattern	olus Ambient (CCIR) NUCOM plus interpretation aircraft systems	None None
Propagation	Ambient virtual- geometry ray set	Limited 3-D virtual geometry, specified rays	2-D ray trace	NUCOM plus linc-of- sight and ground wave	Virtual geometry, single ray
Nuclear Effects	WEPII	Post- stabilization plus plume	WEPII	WEPII	WEPH
Ionosphere	Two-parameter, day∕night	Multiple- parameter, time/space variable	Multiple- parameter, tíme/space variable	As in NUCOM	Electron- density profile
Code	WRECS	HENET	NUCOM	NUCOM- BREM	WEPII

Even if all current models of nuclear phenomena are assumed to be an integral part of the HF nuclear effects prediction codes listed in Table 2, the uncertainties in those models plus the different approaches to modeling the ambient ionosphere and propagation will undoubtedly lead to different results. Differences due to the nuclear models can be attributed to the following factors:

- Limited quantitative data are available to verify the predictive capability of the nuclear effects models.
- Models of nuclear effects are based on the available empirical data or are even calibrated to that limited data.
 The data base is sufficiently small to make extrapolation of results to different nuclear environments precarious.
- The data base is not large enough to allow statistical treatment of the results.
- WEPH has announced limitations, including uncertainties of 2 to 3 in electron density. These uncertainties have an enormous effect in cases in which marginal system performance is predicted.
- F-region uncertainties relate to the location and concentration of high-altitude ionization and to the effect of mechanical waves generated by a burst.
- The weakest aspect of all HF nuclear effects predictions is the modeling of late-time effects.

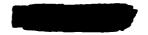
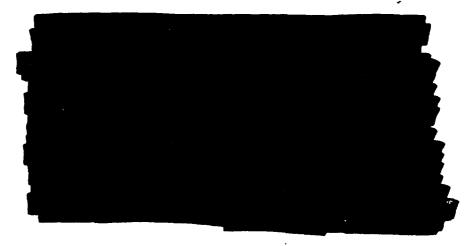


Table 3-3

PREDICTABILITY OF THE EFFECTS OF VARIOUS NUCLEAR PHENOMENA



(b)(i)

B. Prompt Radiation

X-radiation from high-altitude bursts can produce blackout conditions for paths where rays intersect the D region within optical line-of-sight of the burst. The extent of the blackout effects is not a strong function of yield but depends mainly on the burst altitude, as indicated in Figure 10. For example, a 10-MT detonation at 100 km would produce nighttime blackout conditions over an area defined by a radius of about 1000 km; a 10-kT detonation would produce comparable effects over an area defined by a 700-km radius. The duration of blackout from prompt radiation strongly depends on available frequencies and path-burst configuration, but will generally be on the order of a minute at night and 10 to 15 minutes during the day.



81

Pages 82 through 84 were deleted.

(6)(1)

The impact of prompt radiation on the lowest observed frequency (LOF) can be seen from data shown in Figure 12. Predicted and measured values of LOF are given for three paths--Canton to Hawaii, Canton to Midway, and Roi Namur to Hawaii--following three events--CHECK MATE, KING FISH, and STAR FISH. The sharp decreases in LOF during the first few minutes are due to X-radiation. Isolation of this single effect from other causes of absorption requires either substantial displacement of the path from the burst or a small yield such as CHECK MATE. As can be seen from Figure 12, X-rays do not appear as important as other radiation sources in this set of examples. Errors in estimating the LOF are frequent and occasionally significant. Difficulty is likely due to uncertainties in debris location (the source of delayed gamma radiation) and the fact that the LOF is in part a function of system sensitivity, which may be imprecisely known in a step-frequency sounder such as those employed.

C. Delayed Gamma Rays

The HF signal absorption resulting from delayed gamma rays is reasonably well understood and predictable. The predictability of onset time, radial extent, and magnitude of the effects largely depends on the models of fireball/debris dynamics. The maximum extent of gamma ray induced absorption includes all regions where the gamma radiation sources are above 20 km and within line-of-sight of the D region. The magnitude and duration of the effects are estimated as functions of altitude/yield in Figure 13 for day and night conditions. "Outage" on these figures is loosely defined as a condition in which 15-MHz signals would incur 40-dB excess attenuation on two D-region traversals. Clearly, only relatively high-yield, high-altitude bursts are capable of producing extended HF blackout conditions as a result of gamma radiation. However, the ion-production rates from multiple bursts are additive, and the resultant absorption following multiple bursts would be significantly greater than shown on Figure 13, which assumes single-burst conditions.

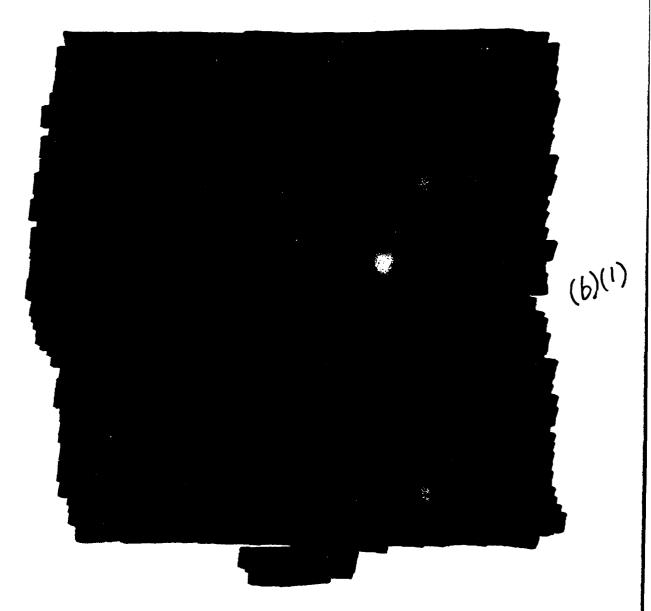


FIGURE 3-13 HEIGHT/YIELD COMBINATIONS REQUIRED TO MAINTAIN OUTAGE AT DISTANCES WITHIN LINE-OF-SIGHT OF THE DEBRIS FOR THE FIRST 30 MINUTES

D. <u>Delayed Beta Particles</u>

Beta-produced ionization resulting from debris decay is the dominant but perhaps the least predictable nuclear effect on HF propagation. The beta-particle-induced ionization from single high-altitude detonations has been observed to produce severe D-region absorption and

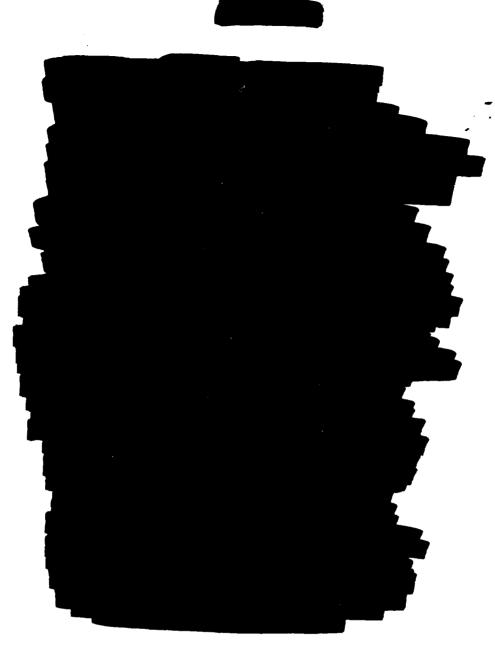


FIGURE 3-14 COMPARISON OF OBSERVED AND COMPUTED GAMMA-RAY INDUCED ABSORPTION

blackout for many hours over extended regions. In fact, computations suggest that in the presence of both gamma rays and beta-induced ionization, the HF signal absorption due to gamma rays is almost insignificant (Figure 15).

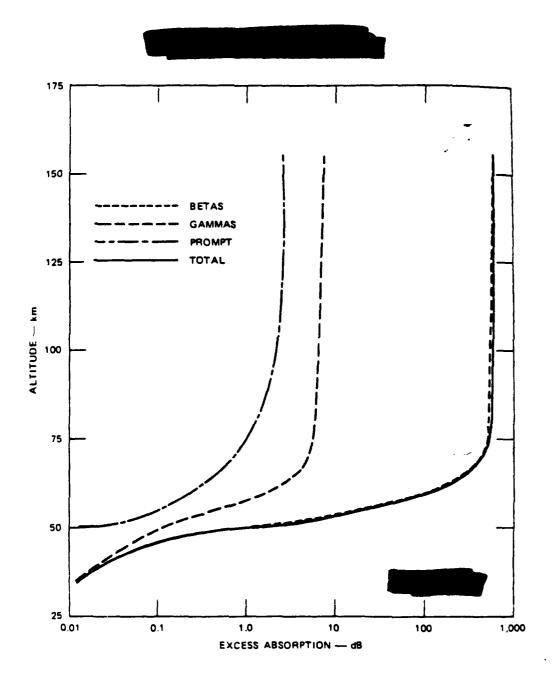


FIGURE 3-15 ONE-WAY-VERTICAL EXCESS ABSORPTION AT 15 MHz
RESULTING FROM BETA, GAMMA, AND PROMPT
RADIATIONS--H + 15 min

The excess vertical absorption shown in Figure 15 was computed for a location 800 km from the burst 15 minutes after burst. The absorption results from a 1-MT, 50 percent fission yield weapon detonated at 100 km within the region illuminated by all three radiation sources. Beta-produced absorption is about two orders of magnitude greater than

absorption due to gamma rays. Since both radiations decrease in intensity approximately inversely with time, the absorption in regions illuminated by beta particles will persist long after gamma ray effects have become inconsequential. Not all nuclear detonations cause beta-induced D-region absorption; to do so a burst must have an altitude/yield combination sufficiently high for the debris to stabilize at altitudes above 60 km, the beta containment altitude.

Unfortunately, the most predictable aspect of beta ionization is whether a given yield/altitude combination will create it. Prediction of the location, magnitude, and duration of the HF degradation can, at best, be termed difficult because of two unrelated sets of problems:

- (1) Problems associated with modeling of the fireball-debris dynamics, since they establish the post-stabilization conditions of the debris volume--altitude, radius, and distribution. The results of any computations are extremely sensitive to the debris models, which precisely define the predicted region of intense beta-produced D-region absorption. Furthermore, in most situations, predictions of the presence or absence of beta-induced D-region absorption is the dominant factor in determining the status of an HF circuit.
- (2) Problems associated with prediction of the poststabilization debris dispersion and motions resulting from
 high-altitude winds. Wind models developed from meteorologic data are expected to provide a statistical representation of the prevailing wind patterns and their effects on
 the debris motions. However--and this is the crux of much
 of the controversy regarding the status of HF in a nuclear
 environment--it is impossible for a statistical representation of the winds to provide results that are appropriate
 for a specific day. Accordingly, predictions of late-time
 D-region absorption effects cannot be expected to compare
 with specific measured propagation data; they can only be
 expected to portray conditions that might have existed on
 an average day.

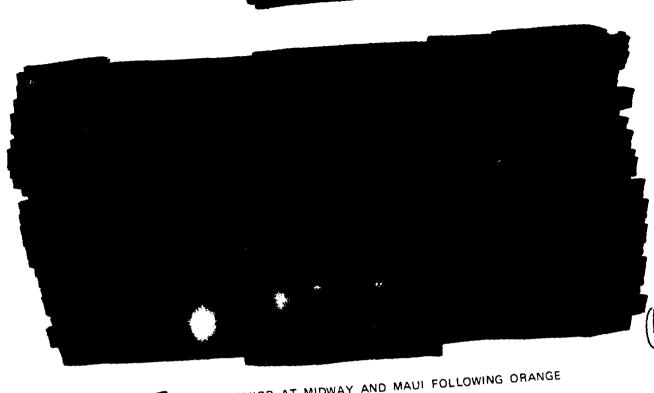
Some of the problems associated with the models of late-time debris location are due to the few high-altitude detonations with yield sufficient to produce measurable beta ionization over wide geographic areas for long durations. This lack of data on which to base a model can be explained by the geography in the Pacific Basin. French Frigate Shoals-about 600 km north of Johnston Island--Hawaii, and Midway--about 1400 km

from Johnston Island--were the nearest land masses from which measurements could be taken. The long-term requirement for inferring debris location from HF measurement data exists because the U.S. high-altitude detonations occurred at night, when the absorption effects recover on the order of 20 times faster than they do during the daytime. Thus, in the case of low-yield high-altitude detonations, beta ionization cannot be detected at night over large areas due to the rapid recovery rates, or during the following day because of dispersion over still greater areas and the radio-active decay that occurs during the additional time.

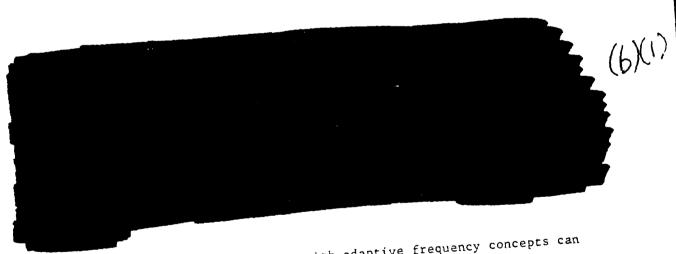
Only four detonations were of sufficient yield to satisfy the above criteria. They were the TEAK and ORANGE events in the 1958 nuclear test series and two of the Soviet shots of 1962.



Page 92 was deleted. (b)(1)



fmin BEHAVIOR AT MIDWAY AND MAUL FOLLOWING ORANGE FIGURE 3-17



New-generation HF systems with adaptive frequency concepts can find paths of opportunity through such potential holes. However, we are not aware of any techniques that can be used to describe analytically their spatial and temporal characteristics. The existence and utility of such holes, if they exist, is likely to diminish in a multiburst environment,

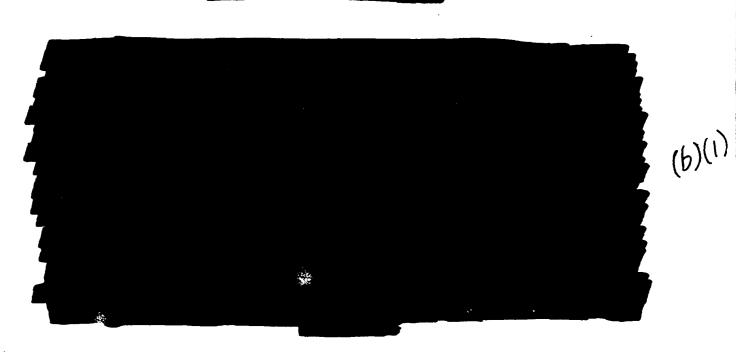
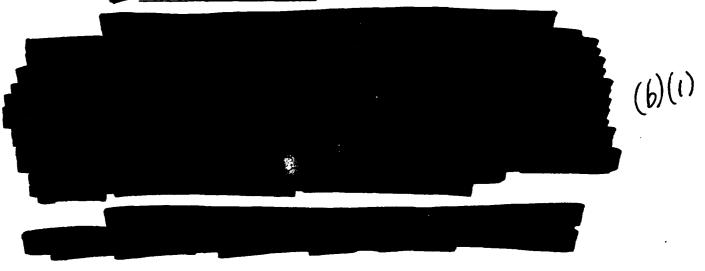


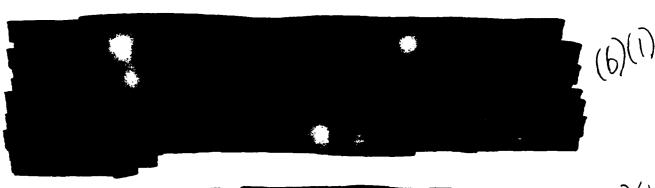
FIGURE 3-20 fmin BEHAVIOR AT TOMSK FOLLOWING OCTOBER 1962 EVENT

where the debris from other bursts should tend to fill the gaps and leave a more uniform debris distribution.

E. Nuclear-Induced F-Region Changes

1. Ionospheric Wave Motion







It is not known whether the interactions of the shock wave with the ionosphere are primarily chemical, mechanical, or both. Chemical effects are certainly important out to some distance, but the data discussed above suggest that a wave motion may be at least partially responsible.

Changes in the F region due to shock and acoustic waves are significant; however, adequate theory has not been developed to model the source functions of these waves as functions of burst altitude and yield. The mechanical wave effects on the F region are modeled empirically

and are based on the small amount of data obtained during the 1958 and 1962 nuclear test series. 18

It is not the mechanical waves but the effect of the waves that is modeled. Changes to layer critical frequency and height are made directly without intermediate wave equations. The technique is to implement empirical data by using a correction factor that has a form and velocity characteristic of the wave. The correction factor itself is partly theoretical and is modulated by two half-cycles of a sunusoid.

In keeping with the effects following TEAK, the shock wave is modeled simply as a step depletion in f_0F2 to 2 MHz that begins at the burst point and travels at a supersonic velocity to a specified distance, after which it is assumed to travel at an acoustic velocity. The shockwave velocity is then decayed exponentially to an acoustic velocity at a range of R_A . The assumed manner in which the transition from a shock wave to an acoustic gravity wave is made is shown in Figure 22. The exponential is defined by the initial slope of the range-versus-time curve (mach number) and the constraint that the slope at t_A must be the acoustic velocity of the peak of the first half-cycle of the wave.

Once the shock wave has degenerated into an acoustic gravity wave (by some mechanism not yet fully understood), the changes are believed to be caused entirely by the mechanical effects of moving air, including the consequent turbulence and heating. As the wave passes an observation point, the F-region critical frequency increases and then decreases, or vice versa.

when a nuclear explosion occurs in the northern geomagnetic hemisphere, the region north of the detonation will experience an initial increase in F-region critical frequency, the region between the burst and the geomagnetic equator will experience an initial decrease, and the region south of the magnetic equator will experience an initial increase. Figure 23 shows the regions of critical-frequency increase and decrease during the first half-cycle of the wave for nuclear detonations at Johnston Island. During the second half-cycle of the wave, the changes in critical frequency will be in the opposite direction.

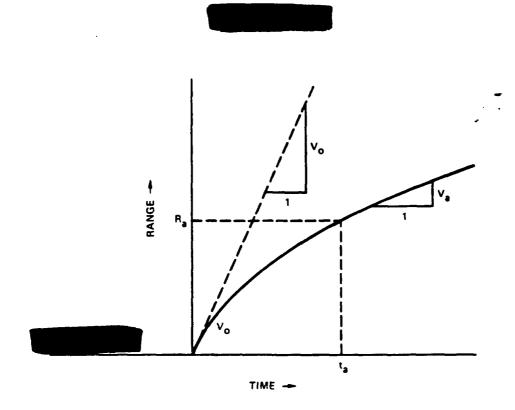
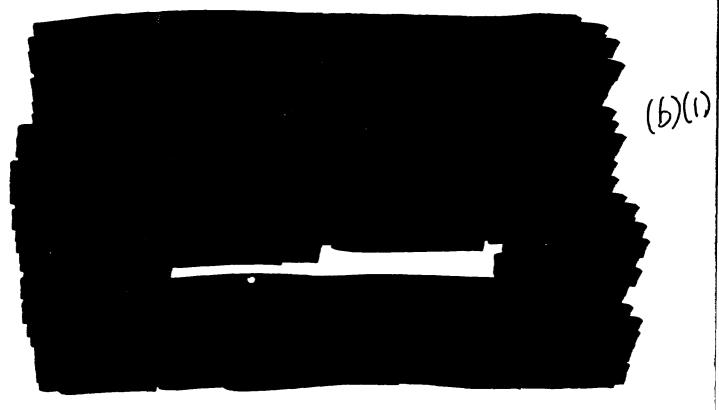
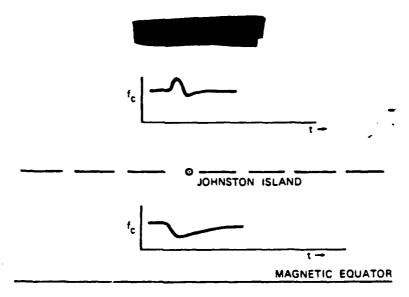


FIGURE 3-22 TRANSITION FROM INITIAL TO ACOUSTIC-WAVE VELOCITY





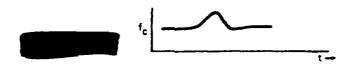
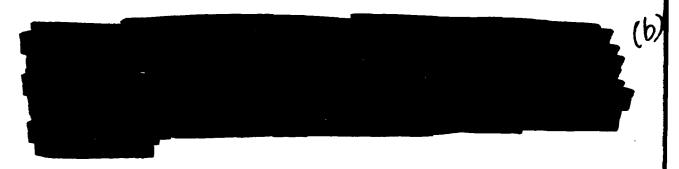


FIGURE 3-23 GEOMAGNETIC FIELD DEPENDENCE OF ACOUSTIC-GRAVITY WAVE



2. High Altitude Ionization

One of the most spectacular results of the HF propagation experiments during the 1962 high-altitude nuclear test series was the observation of anomalous modes on many of the paths. These modes were created by scattering from high-altitude ionization that had been produced by the burst and spread preferentially along the earth's magnetic field; the scatterers extended from the vicinity of the burst to both conjugate regions. The off-path modes were observed in the upper HF and

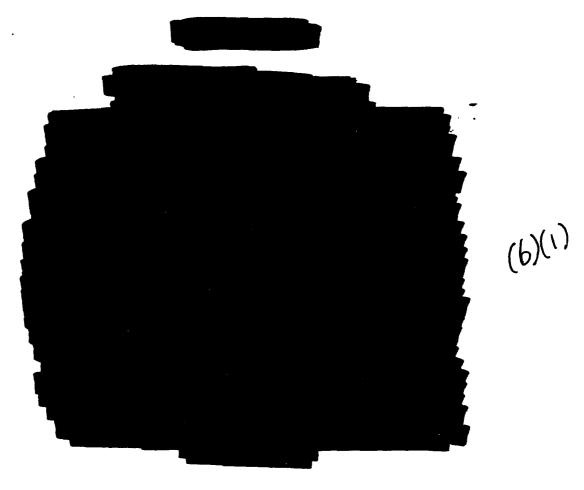


FIGURE 3-24 IONOSPHERIC WAVE POSITION vs. TIME FOLLOWING CHECK MATE

existence on specific paths depended primarily on the geometric relationship between the path and magnetic field. Figure 26 illustrates the equiangular geometry required to produce off-path modes, providing the elongation along the field is long compared to the wavelength. For a maximum reflection coefficient, the receive: must lie along the intersection of the illustrated cones and the earth's surface.

The particular angle of the magnetic field in the vicinity of the 1962 Johnston Island tests favored this type of reflection mechanism. From that experience came the idea that such modes were a natural adjunct to communications in a nuclear environment, but this concept is not accurate. Certain paths in the 1962 tests can be used to illustrate this.

Page 103 was deleted. (b)(1)

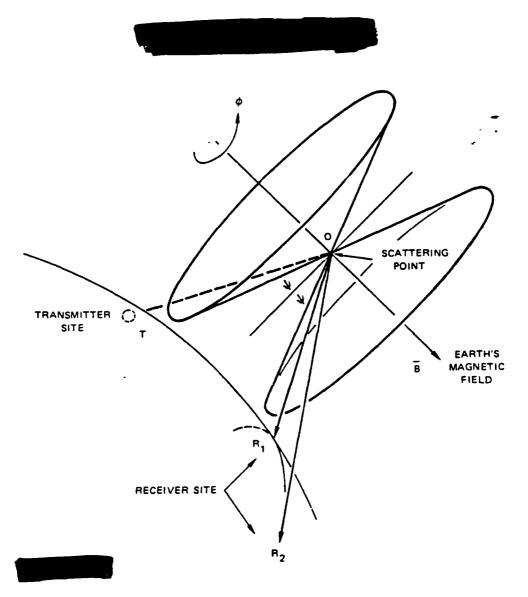


FIGURE 3-26. EQUIANGULAR SCATTERING GEOMETRY



Pages 105 through 107 were deleted (b)(1)

104

. 4

VI CONCLUSIONS

The role, or potential role, of HF systems as part of a survivable communication network has been a subject of debate and controversy within the DoD since the first high-altitude nuclear detonation. As with many other systems operating in other frequency bands, the performance of HF systems in a nuclear environment is extremely sensitive to scenario conditions. In fact, slight variations in any of a number of important parameters can often have a profound effect on the prediction results for a specific situation. Accordingly, this sensitivity of predictions or measurements to slight changes in parameters makes any evaluation of our prediction capability a formidable task.

In the process of assessing our overall predictive ability, we have discussed the characteristics of the necessary models and have given some examples of predictions and measurements. In particular, we have briefly described the status of modeling and predicting:

- Ambient ionospheric conditions
- Ambient propagation conditions
- Nuclear effects on the propagation medium, including:
 - Prompt radiation
 - Delayed gamma radiation
 - Delayed beta particle radiation
 - High-altitude ionization
 - Traveling disturbances.

We have tried to identify situations and phenomena in which high confidence predictions are attainable and those in which major uncertainties exist.

Analysis of measurements and predictions suggests that the best ambient ionospheric and propagation models adequately portray median ionospheric and propagation conditions. On the other hand, ionospheric models do not usually portray the naturally occurring variations about the median

values of, for example, the maximum frequency. Since upper decile MOF values may typically translate into frequency support on the order of 30 percent higher than at the median, such models might present a somewhat more favorable estimate of survivability for systems that employ adaptive frequency concepts. Unfortunately, there are a number of uncertainties in determining the appropriate spatial and temporal correlations of these naturally occurring ionospheric variations. Any analysis of systems using adaptive frequency concepts must somehow account for not only the naturally occurring but also the nuclear-induced variations before realistic estimates of the potentially available frequencies can be made.

Comparing measurements with predictions for the specific weaponinduced degradations suggests that the prompt and gamma radiation effects
are well understood and quite predictable, as are the major features of
ionospheric wave effects from a single detonation at long ranges. The
occurrence of intense burst-induced ionization aligned with the magnetic
field and creating off-path (VHF) propagation modes is predictable. The
utility of such modes is generally confined to lower latitudes; it is
marginal at higher latitudes. Even at lower latitudes, predictions of
the duration and cross-sections for such modes are inadequate. Because
of the difficulty in predicting debris distribution at late times, the
corresponding absorption effects of beta-produced ionization are also
difficult to predict. Since the cause of the F-region depletion is not
understood, its extent and magnitude are also difficult to predict.

These variations in predictability produce striking contrasts in the believability of prediction results, the contrasts extending into different space and time regimes and scenario conditions. This fact, coupled with the sensitivity of prediction results to the other critical parameters in predicting HF performance, strongly suggests that prediction results are only indicative of conditions that could exist. Results must be interpreted in terms of uncertainties associated with both the scenario and the prediction models. In spite of their shortcomings the prediction codes remain the best available tool for estimating either HF system or network performance in a nuclear environment. Otherwise HF performance estimates cannot be generalized beyond these broad statements:

Page 110 was deleted.

(b)(i)



- 1. W. J. Russell, Jr., S. Perlman, and S. E. Probst, "Effects of High Altitude Detonations on High Frequency Communications "U.S. Army Signal Radio Propagation Agency, Fort Monmouth, NJ (August 1959),
- 2. H. L. Kitts, J. B. Lomax, et al., "Project Officer's Interim Report-Project 6.11, HF Communications Experiment "," Project Officer's Interim Report Operation Dominic, Fish Bowl Series (December 1962),
- 3. H. L. Kitts and J. B. Lomax, "Project Officer's Report, Volume 1, Project 6.11, HF Communications Experiment," (April 1964), POR-2030,
- 4. D. L. Nielson, "HF Communications Related to the Soviet High-Altitude Bursts", "Contract No. DNA001-73-C-0180, Published in Proceedings of the DNA 1973 Atmospheric Effects Symposium Vol. VI, DNA 3131 P-6, Stanford Research Institute, Menlo Park, California (June 1973), "California".
- 5. W. S. Knapp, "A Simplified D-Region Chemistry Model for Nuclear Environments"," DNA 2850T, Contract DASA01-69-C-0132, GE TEMPO, Santa Barbara, California (April 1972),
- D. L. Nielson, "Anomalous HF/VHF Propagation Modes During Fish Bowl DASA 1599, AD-359 8746, Contract DA 36-039 SC-87197, Stanford Research Institute, Menlo Park, California (January 1965),
- 7. J. N. Freedman, "Reassessment of HF Propagation in a Nuclear Environment," Mitre Technical Report 2646, Vol. II, ESD Contract F19 (628)-73-C-001, The Mitre Corporation, Bedford, MA (September 1973),
- *8. "Advanced MEECN High Frequency Communication System Concept Formulation ," Technical Publication TP 11-76, Defense Communication Agency, Arlington, VA (May 1976),
 - 9. D. L. Lucas, G. Haydon, et al., "Predicting Statistical Performance Indexes of High-Frequency Ionospheric Telecommunication Systems," Technical Report ITSA-1, Institute for Telecommunication Sciences and Aeronomy, Boulder, Colorado (1966).

- 10. T. Elkins and C. Rush, "A Statistical Predictive Model of the Polar Ionosphere," in T. Elkins, ed., An Empirical Model of the Polar Ionosphere, AFCRL-TR-73-0331, Air Force Cambridge Research Laboratories, L. G. Hanscom Field, Bedford, MA, 1973.
- 11. R. R. Vondrak, G. Smith, V. E. Hatfield, R. T. Tsunoda, V. R. Frank, and P. D. Perrault, "Chatanika Model of the High-Latitude Ionosphere for Application to HF Propagation Prediction," RADC-TR-78-7, Final Report, Contract F19628-77-C-0102, SRI International, Menlo Park, CA 94025 (January 1978),
- 12. T. I. Dayharsh, "HF Communications Effects: Ionospheric and Mode of Propagation Measurements"," DASA 1701, Final Report, Contract DA 36-039 SC-87197, Stanford Research Institute, Menlo Park, CA 94025 (August 1965),
- 13. D. L. Nielson, J. B. Lomax, and H. A. Turner, "The Prediction of Nuclear Effects on HF Communications," DASA 2035, Final Report, Contract DA-49-XZ-436, Stanford Research Institute, Menlo Park, CA 94025 (November 1967).
- 14. R. A. Demarest and T. I. Dayharsh, "Propagation Plots Derived from Oblique-Incidence Ionograms--Okinawa to Saigon," Final Report, SRI Project 5663, Contract CST-7681, Stanford Research Institute, Menlo Park, CA (November 1965).
- 15. W. S. Knapp and K. Schwarz, "WEPH VI: A FORTRAN Code for the Calculation of Ionization and Electromagnetic Propagation Effects Due to Nuclear Detonations: Volume 1, User's Manual "," DNA 3766T-1, Topical Report, Contract DNA001-75-C-0096, General Electric Company-TEMPO, Santa Barbara, CA (September 1975),
- 16. E. J. Feniger, "WRECS VI Code: A FORTRAN Code for the Computation of Weapon Radiation Effects on Communication Systems," DCA 100-74-6-0021, DCA 100-75-C-0010, General Electric Company-TEMPO, Santa Barbara, CA (June 1975),
- 17. D. H. Sowle, "An Ambient HF Radio Mode Model (U)," DNA 4420T, Topical Report, Contract DNA 001-76-C-0349, Mission Research Corporation, Santa Barbara, CA (September 1977),
- 18. E. J. Baumann, V. E. Hatfield, and J. Owen, "Documentation of NUCOM II--An Updated HF Nuclear Effects Code," DNA3108F1, Final Report, Contract DASA01-71-C-0138, Stanford Research Institute, Menlo Park, CA (April 1973),
- 19. G. P. Nelson, "NUCOM/BREM: An Improved HF Propagation Code for Ambient and Nuclear Stressed Environments," DNA 4248T, Final Report, Contract DNA 001-76-C-0261. GTE Sylvania, 189 "B" Street, Needham Heights, MA (October 1976),

- 20. E. J. Baumann, G. H. Smith, D. L. Nielson, and W. E. Jaye, "An Overview of HF Communications in a Nuclear Environment," DNA 3301T, Special Report 1, Contract DNA001-73-C-0180, Stanford Research Institute, Menlo Park, CA (March 1974),
- 21. G. H. Smith, "An Introduction to OTH Radar Performance in a Nuclear Environment," DNA 3736T, Topical Report 3, Contract DNA001-73-C-0180, Stanford Research Institute, Menlo Park, CA (May 1975),
- 22. H. F. Busch and A. Kavka, "Some Effects of High Altitude Nuclear Detonations on the Ionosphere During Project Newsreel, Operation Hard Tack," Project 678 Interim Report, U.S. Army Signal Radio Propagation Agency, Fort Monmouth, NJ (March 1959),
- 23. W. F. Utlaut, "Ionospheric Effects Due to Nuclear Explosions,"
 NBS Report 6050, Project 8520-12-8510, NBS Boulder Laboratories,
 Boulder, CO (April 30, 1959).
- 24. L. T. Dolphin and R. B. Dyce, "Operation Hardtack/Newsreel Radio Attenuation and Reflection Phenomena "," Contract SRI Project 2445, Stanford Research Institute, Menlo Park, CA (February 1960),
- 25. H. F. Busch, "A Preliminary Review of Russian Ionosonde Observations," External Tech. Mem. 79, ITT Electro-Physics Labs., Inc., Columbia, MD (April 1968),
- J. B. Lomax and D. L. Nielson, "Observation of Acoustic-Gravity Wave Effects Showing Geomagnetic Field Dependence," J. Atmos. Terr. Phys., Vol. 30, pp. 1033-1050 (1968),

CHAPTER 4. HF SKYWAVE COMMUNICATIONS ROLE AND THE NUCLEAR ENVIRONMENT

Mr. W. Jaye, SRI International

I

INTRODUCTION

SRI International has been studying and analyzing the effects of high altitude nuclear detonations for DNA for more than 15 years. In the course of the latest effort, under Contract DNA001-77-C-0063, SRI was asked by DNA to evaluate proposed low-data-rate "broadcast" systems that are intended to operate in a severe nuclear environment and that utilize frequencies between 3 MHz and nearly 100 MHz.* Previously, as part of the same contract, SRI had analyzed the performance of rapid two-way communication systems in a recovering nuclear environment.*

Under separate contracts, SRI had the opportunity to study the performance of the World Wide Military Command and Control System (WWMCCS) in a severe nuclear environment. These studies covered the time periods of the attack, the immediate trans-attack period, and the time frame when restoration of communications and reconstitution of forces are of prime importance--namely, two to seven days after a severe nuclear laydown.

The basic conclusions that we have reached as the result of these studies are: that HF communications systems are needed in the tracture of the WWMCCS in order to provide the necessary post-attack communications capability, and that new system concepts and operational doctrines are required to make HF communications as efficient and timely as possible. In particular, it is necessary to provide these HF communications systems with frequency versatility and agility, and to extend their operating range to the high MF and low VHF range.

5 174995171

W. A. Edson and G. H. Smith, "HF Systems for MEECN Applications and Enduring Communications"," DNA 4646, Topical Report 1, Contract DNA 001-77-C-0063, SRI International, Menlo Park, CA (June 1978),

T. W. Washburn and G. H. Smith, "Adaptable Communication Systems for use in a Nuclear Environment "DNA 3796T, Topical Report, Contract DNA001-73-C-0180, SRI International, Menlo Park, CA (September 1975),

G. R. Underhill et al., "WWMCCS Performance in a Severe Nuclear Environment", DNA 3659F, Technical Report 1, Contract DNA001-74-C-0271, SRI International, Menlo Park, CA (March 1975),



- A Directed Program to Develop HF Propagation Management Technology Should be Initiated.
- ▲ Methods to Restore Communications and Reestablish Connectivity Should be Evaluated.
- ▶ Procedures, Operational Protocol, Required Flexibility, Redundancy, etc., Should be Defined.
- Gaps in Knowledge of Propagation Phenomenology in a Trans-and Post-Nuclear Environment Should be Assessed and Steps Taken to Reduce Uncertainties.

CHAPTER 5. LOW DATA-RATE GROUNDWAVE COMMUNICATIONS *-

Dr. C. Crain, The Rand Corporation

I. INTRODUCTION

The purpose of this report is to present a general indication of the communication capabilities which can be achieved at frequencies in the high frequency band (3-30 MHz) and below, if signal propagation is only by the ground wave mode. Signal propagation for the ranges to be considered (i.e., less than 1000 miles) is normally influenced, if not controlled, by ionospheric reflection. Practical experience with only ground wave communications at large distances is generally lacking. One can use the results of this note to partially answer questions such as "what communication capability would exist if there were no ionosphere of if radio signal transmission via the ionosphere were completely absorbed?" In this report emphasis is placed on propagation and noise considerations. Such terminal factors as antenna types, transmitter power levels achievable at a given frequency, and overall transmitter costs for a prescribed effective radiated power are not considered. Assessment of these factors coupled with the material presented will provide a basis for determining the practicality of achieving a suggested dual system capability ** and for optimum design of the system.

II. GENERAL PROPAGATION CONSIDERATIONS

At frequencies in the high frequency band and below, the transmission of radio signals between a transmitter and beyond-the-horizon receivers occurs principally by ground wave propagation, ionospheric

The work was done under a program supported by the Defense Nuclear Agency under NWED Subtask Code S99QAXHEO, Work Unit Code 23.

i.e., one that gives reliable very low data rate transmission during conditions of very poor or negligible ionospheric transmissions and also provides reliable voice communications during normal conditions.

reflection, or a combination of both. Under normal ionospheric conditions the signal received via ionospheric reflection becomes stronger than the ground wave signal beyond a certain distance depending on frequency, time of day, and the nature of the surface (i.e., sea water, smooth terrain, mountain terrain, etc.), sunspot number, polarization, etc.

Figure 1 shows the approximate distance from the transmitter at which the ground wave signal and the sky wave signal are of equal amplitude as a function of frequency, for frequencies between 0.1 MHz and 30 MHz, and for the conditions prescribed, i.e., mid-day, over land with typical electrical properties, and an average sunspot minimum ionosphere. Between about 1 MHz and 10 MHz a band of ranges is shown reflecting the sensitivity of the ionospheric signal to details of the ionosphere structure which can occur. Above 10 MHz the ionospheric signal, for the ranges involved, is due to ionospheric scatter. At night, ionospheric signals, for the frequencies and ranges of Figure 1, are larger; hence Figure 1 can be interpreted as showing average expected maximum distances for which the ground wave signal is equal to a typically expected ionospheric signal. For example, at 1 MHz, during daytime, Figure 1 shows the ground wave signal to be greater than the ionospheric signal to distances of 300 miles. At night this distance would typically be in the vicinity of 50 miles.

Since the objective of this report is to examine the possible communications capabilities using only the ground wave signal, Figure 1 is presented only to provide a degree of perspective relative to normal experiences. For example, 1 MHz signals, if received during mid-day at distances out to 300 miles, are normally propagated via the ground wave mode while those beyond about 300 miles are due to ionospheric propagation. Similarly, at 10 MHz any received signal out to about 100 miles would normally be due to ground wave propagation. What Figure 1 does not indicate are system parameters necessary to provide a specified

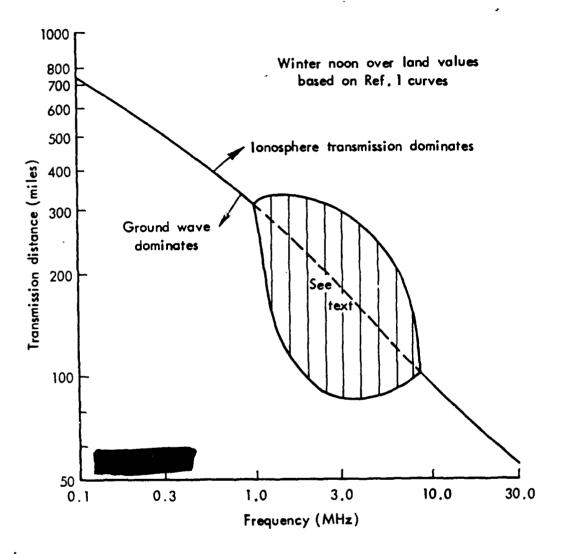


Fig. 5-1 Comparative ground wave and ionospheric transmission

communication capability at any frequency or distance. This we will next discuss.

III. GROUND WAVE PROPAGATION OVER LAND

The decrease in ground wave signal intensity with distance from a transmitter is well established, theoretically and experimentally, for an ideal spherical earth of specified electrical properties. Certain practical aspects such as variability of the electrical constants of the earth along the path or with depth, terrain of varying degrees of roughness, forests, etc. cause some departure from ideal calculated characteristics; however, for present purposes these effects will be ignored and deductions will be based on the use of standard published basic transmission loss curves such as are given in any radio propagation textbook or handbook. The particular loss curves used in this note were taken from Ref. 1. Basic transmission loss as defined in Ref. 1 and used in this note is simply

$$L_b = 10 \log_{10} (p_t/p_r)$$
 (1)

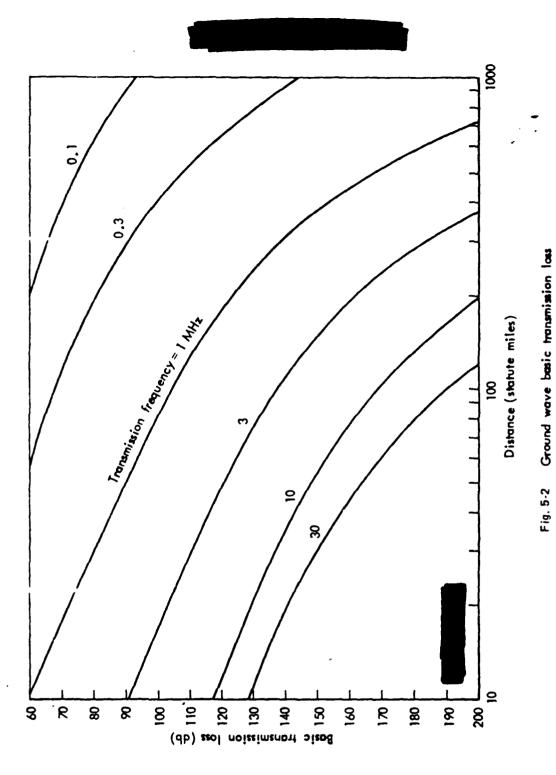
where p_t is defined as power radiated by an isotropic antenna and p_r is the power delivered by a loss-free isotropic receiving antenna.

For real antennas having gain in the transmission path direction Eq. (1) becomes

$$L = L_b - G \tag{2}$$

where G is the summed transmitting and receiving antenna gain, in decibels, along the transmission path. It should be noted that L_b is defined as a positive number of decibels. For real antennas with loss, Eq. (2) can be modified directly to account for such loss.

Figure 2 shows for frequencies between 0.1 MHz and 30 MHz basic



transmission loss for a smooth spherical earth (conductivity 0.005 mho/meter and dielectric constant = 15) as a function of distance in statute miles.

As an example, let us use Figure 2 to determine the signal power delivered by an isotropic receiving antenna at a distance of 100 miles from an isotropic transmitting antenna which radiates 1 watt at a frequency of 1 MHz. Figure 2 shows the basic transmission loss to be 105 dB, thus for p_{+} = 1 watt

$$\log \frac{1}{p_r} = 10.5 \text{ or } \frac{1}{p_r} = 3.16 \times 10^{10} \text{ or } p_r = 3.16 \times 10^{-11} \text{ watts}$$
 (3)

The result (3) can be modified directly to account for receiving antenna loss and total (transmitting and receiving) antenna path gain. In this note neither of these factors is included in the results presented. The results can be quite simply adjusted to incorporate any specific antenna parameters.

IV. NOISE

The desired signal level necessary for satisfactory reception is determined by the level of competing undesired signals in the receiver pass band and internal receiver noise. Undesired signals at the receiving antenna are normally considered to be due to four sources as follows:

- (1) Galactic or cosmic radio noise.
- (2) Noise produced by lightning and propagated via the ionosphere or ground wave to the antenna.
- (3) Other intentionally generated radio transmissions in the receiver band.
- (4) All other noise produced by man-made devices such as automobiles, transmission lines, industrial equipment, etc.

Under normal conditions of ionospheric propagation, noise of a given frequency is propagated the same as signal at that frequency. Since this note is concerned with the ultimate capability of a ground wave only communications system under conditions of unusually severe absorption of the ionospheric signal, noise considerations are different from those normally used. If no desired signal is transmitted via the ionosphere, we will assume also that no noise reaches the receivers via ionospheric transmissions. Thus source (1) noise is eliminated and source (2) noise is only that reaching the antenna via ground wave propagation. Source (3) noise is restricted, in general, to transmitters within ground wave range of the receiver. Source (4) noise is unaffected, in general, since this noise normally arises from man-made sources near the receiver.

Despite elimination of consideration of noise propagated via the ionosphere, specifying noise levels appropriate for system capability assessments can at best be only approximate and for the most part arbitrary. Man-made noise varies widely with location and even at a given location there is often wide variability with time. Atmospheric noise from lightning propagated by ground wave will reach the receiver. The level and occurrence of such noise, in general, will vary widely and can only be described statistically (time of day, season, etc.) much the same as is done for the case of normal ionospheric propagation in Ref. 2. In order to provide first order quantitative values we have arbitrarily chosen for expected noise the values presented in Ref. 2 for expected man-made noise at a "quiet" receiving location. Figure 3 shows this noise level, expressed in dB above thermal noise for the frequency range we are considering; if one has receiver locations which are "very quiet" the true system noise could be much less than Figure 3 and deductions based on Figure 3 would need appropriate modification. Also, if noise-suppression techniques can be applied to man-made noise,

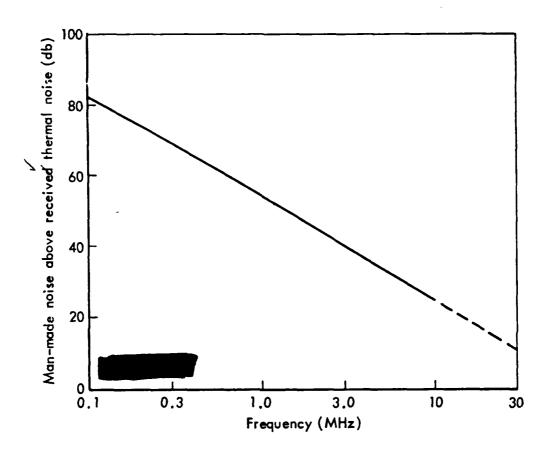
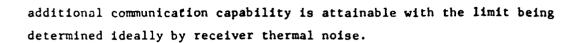


Fig. 5-3 CCIR quiet man-made noise levels (Ref. 2)



V. GROUND WAVE SYSTEM CAPABILITY ASSESSMENT

Using the ground rules discussed in Sections III and IV, i.e., only ground wave signal propagation and noise levels appropriate for so-called "quiet" man-made noise as shown in Figure 3, one can readily provide results expressed as signal-to-noise ratio useful for estimating attainable system capability.

The signal-to-noise ratio (expressed in dB) is given by

$$S/N_b = P_t - L_b - N_b \tag{4}$$

where $N_{\rm h}$ is the noise in the receiver signal bandwidth (Figure 3)

P is the effective radiated power of the transmitter

 $L_{\rm b}$ is the basic transmission loss (Figure 2)

For numerical values we will use an effective radiated power of 1 kW (30 dB) and a signal bandwidth of 1 Hertz. Using these fixed parameters for illustration, we will calculate the signal-to-noise expected at a distance of 500 miles for a transmitter frequency of 1 MHz. From Figure 2, $L_{\rm b}$ = 169 dB. From Figure 3, the noise level is 54 dB above thermal noise (KTB). Assuming a temperature of 288°K (as used in Ref. 2) and a bandwidth of 1 Hertz

$$KTB = 1.38 \times 10^{-23} \times 288 \times 1 = 3.97 \times 10^{-21} = -204 \text{ dB}$$
 (5)

where K is Boltzmann's constant

T is temperature in degrees Kelvin

B is bandwidth in Hertz

Use of the above values and Eq. (4) gives

(6)

At 300 KHz, for the same conditions, i.e., 1 Hertz bandwidth, 1 kW effective radiated power, and a communication range of 500 miles the result, using Figures 2 and 3 as before, is

$$S/N_b = 30 - 108 - (69 - 204) = 57 dB$$
 (7)

Using the above procedure one obtains Figure 4, which shows for the assumed parameters (1 kW effective radiated power and one Hertz communication bandwidth) the expected receiver signal-to-noise (with the previously given qualifications and assumptions) as a function of transmission frequency for several communication ranges between 100 and 2000 miles. In Figure 5 signal-to-noise is plotted as a function of range for frequencies from 0.1 to 10 MHz.

For comparison of the results in Figure 5 with nominal capability using the same transmitter power under favorable ionospheric conditions * for 1 MHz propagation (signal and noise), L, would typically be near 100 dB for distances of about 200 to 1000 miles (Ref. 1, Figure 41) and N_h would be expected to be less than about 80 dB above KTB for an estimated 99 percent of the time in mid-latitudes. Thus

$$S/N_b = 30 - 100 - (80 - 204) = 54 dB$$
 (8)

for 1 Hertz bandwidth.

Under these conditions the same assumed facilities could provide, say, 1000 Hertz bandwidth communications with a signal-to-noise ratio of 54 - 30 or 24 dB for ranges to about 1000 miles. At times when,

i.e., at night. During day favorable conditions occur for higher frequencies.



1 Kw erp 1 Hertz bandwidth CCIR quiet man-made noise

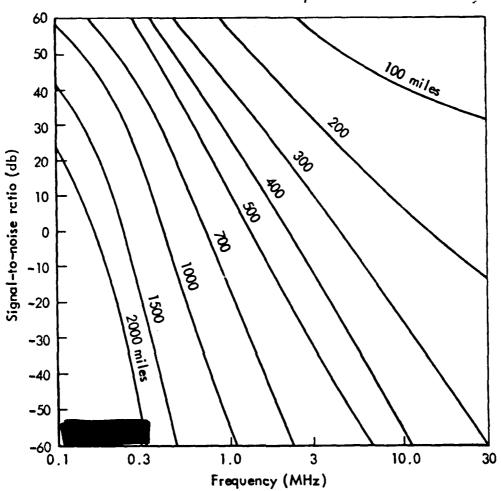


Fig. 5-4 Signal to-noise ratio vs frequency (ground wave transmission over land)

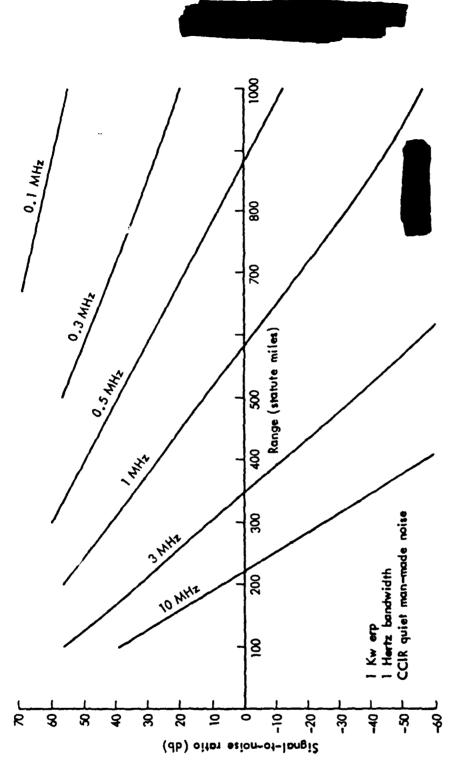


Fig. 5-5 · Signal-to-noise ratio vs range -- ground wave transmission overland

say, 10 MHz is the optimum transmission frequency to a distance of, say, 1000 miles, about the same capability exists for the same assumed terminal parameters. One can verify by study of typical normal ionosphere transmission loss curves such as given in Ref. 1 that the terminal parameters assumed would provide reliable voice communications to 1000 mile range by the appropriate choice of frequency (day or night) and a useful capability (about 10 dB less) at ranges to 2000 miles.

Under conditions of no ionospheric transmission, Figures 4 and 5 indicate that, if one requires communication via ground wave transmission, the achievable range is very sensitive to frequency and that, for a given effective radiated power, frequencies below, say, 1 MHz are much more attractive than frequencies above 1 MHz. Consider, for example, a desired range of 500 miles. From Figure 5 one sees that ground wave transmission at 0.5 MHz is 75 dB better than transmission at 3.0 MHz. As discussed earlier, one needs to know the relative difficulty of obtaining a given level of effective radiated power as a function of frequency before full assessment of the best frequency choice for a desired capability can be made; however, clearly the 75 dB transmission advantage at 0.5 MHz relative to 3.0 MHz will swamp any antenna considerations. For ranges greater than 500 miles the lower frequencies are even more attractive relative to the higher frequencies.

VI. CONCLUSIONS

It is feasible using practical terminal parameters and ground wave transmissions to obtain very low data rate communications over land between terminals spaced up to distances of 1000 miles or more (over water is more favorable) at frequencies which normally depend on the ionosphere for signal transmission—if signals normally transmitted via the ionosphere are assumed to be completely absorbed. For obtaining a reliable over land capability at the longer ranges, say 500 to 1000

miles, it is necessary assuming modest transmitter power (as illustrated by Figure 5) to use transmission frequencies below about 1 MHz. At frequencies of 0.1 to 1 MHz, a good capability appears attainable if one provides an effective radiated power from the transmitting antenna of the order of 10 to 1000 watts depending on frequency and desired range.

The same general facilities which can provide a useful low data rate capability, say I bit per second, to distances of 500 to 1000 miles under the condition of complete loss of ionospheric transmission should provide reliable voice communications for normal ionospheric propagation conditions to receivers at this range. For normal conditions, the ground wave communications capability expected for conditions of loss of ionospheric transmission is greatly reduced, in general, by the increased noise levels.

More effort is required to define optimum antenna and other terminal characteristics for providing the suggested dual capability system, i.e., one that gives reliable low data rate transmission during conditions of very poor or negligible ionospheric transmission and also provides reliable voice communications during normal conditions.

REFERENCES

- 1. Norton, K. A., Transmission Loss in Radio Propagation II, U.S. Department of Commerce, National Bureau of Standards, NBS Report #5092, 1957.
- 2. World Distribution and Characteristics of Atmospheric Radio Noise, International Radio Consultative Committee, Report #322, International Telecommunications Union, Geneva, 1964.